Journal of Applied Polymer Science

Enhancing mechanical properties of aromatic polyamide fibers containing benzimidazole units via temporarily suppressing hydrogen bonding and crystallization

Ke Li, Longbo Luo, Jieyang Huang, Huina Wang, Yan Feng, Xiangyang Liu
State Key Laboratory of Polymer Materials Engineering, College of Polymer Science and Engineering, Sichuan University, Chengdu, Sichuan, People's Republic of China
Correspondence to: X. Liu (E-mail: lxy6912@sina.com)

ABSTRACT: The copolymerization modified poly(p-phenylene terephthalamide) containing 2-(4-aminophenyl)−5-aminobenzimidazole (PABZ) units in the main chain was synthesized and the corresponding poly-p-phenylene-benzimidazole-terephthalamide (PBIA) fibers were prepared by wet spinning. The HCl, the by-product released during polymerization, can complex with PABZ units to prevent the formation of hydrogen bonding between PABZ units, resulting in amorphous PBIA fibers and a lower glass transition temperature (T_g). Therefore, for the purpose of gaining strong hydrogen bonding and high orientation degree at the same time in PBIA fibers, two-step drawing–annealing processing was adopted. The as-spun PBIA/HCl complex fibers were drawn first at 280°C, higher than the T_g of the PBIA/HCl complex fibers and lower than the decomplexed temperature of HCl, which temporarily suppresses the formation of hydrogen bonding and crystallization. Subsequently, the fibers were annealed to reform hydrogen bonding between PABZ units and crystallization via decomplexation of HCl at 400°C. However, when the drawing is above the decomplexed temperature of HCl, the decomplexation of HCl begins to occur which leads to the reform of hydrogen bonding and crystallization, and the tensile strength of the drawn-annealed PBIA/HCl complex fibers decreases with a decrease in the HCl content of fibers. The tensile strength of two-step drawn-annealed fibers increased by approximately 15% compared to that of one-step drawn PBIA/HCl complex fibers. © 2015 Wiley Periodicals, Inc. J. Appl. Polym. Sci. **2015**, *132*, 42482.

KEYWORDS: copolymers; crystallization; polyamides

Received 5 February 2015; accepted 5 May 2015
DOI: 10.1002/app.42482

INTRODUCTION

As we know, the stronger the interaction between polymer macromolecular chains is, the better the mechanical properties of polymers will be. Hydrogen bonding which is found in polyamide fibers and polyvinyl alcohol fibers, resulting in high tensile strength and initial modulus, as the strongest physical interaction, is a useful way to improve the mechanical properties of materials. However, hydrogen bonding also acts like quasi-crosslinks, restricting the movement of molecular chain[1,2] and leading to poor processability. Currently, many researchers have made a great effort to solve contradiction between high performance and good processability.[3,4] Among these methods, temporarily suppressing hydrogen bonding in the processing process and following regeneration of hydrogen bonding in the finished product is an effective way, which can improve the processability without changing their outstanding properties.[5–7] For example, Nishimura *et al.*[5] observed that by complexation with phenyl boronic acid to destroy the hydrogen bonding in poly(vinyl alcohol), poly(vinyl alcohol) can convert into melt flowable derivatives. Afshari *et al.*[6] demonstrated that Lewis acid–base complexation of polyamides provides a way to temporarily suppress hydrogen bonds and crystallinity, potentially increasing the orientation while drawing, following regeneration of hydrogen bonding in the drawn state, to impart higher performance to their fibers.

For the high-performance fibers, the high molecular orientation and crystallization usually corresponds to high mechanical properties. One of the most prominent examples are poly(p-phenylene terephthalamide) (PPTA) fibers. PPTA fibers possess a unique combination of high tensile strength and modulus, toughness, and thermal stability. Due to the structural symmetry and stiffness of the molecule, the spinning solution of PPTA can be converted to liquid crystal solution in high temperature, and the high orientation and crystallization are a direct result of

Additional Supporting Information may be found in the online version of this article.

high levels of molecular alignment achieved through the spinning of liquid crystalline solutions.[8] In the recent years, the PBIA fibers are obtained by introducing 2-(4-aminophenyl)−5-aminobenzimidazole (PABZ) into PPTA main chain.[9] The mechanical properties of PBIA fibers are higher than that of PPTA fibers due to the strong hydrogen bonding between PABZ units.[9] However, due to the lack of symmetry of PABZ and copolymerization, the PBIA fibers cannot be produced through liquid crystal spinning, and such PBIA fibers are less ordered[10] and show lower orientation than that of PPTA.[11] Therefore, the higher mechanical properties of PBIA fibers can be obtained by further improving the orientation degree. Drawing, a processing technique, is often used to enhance the orientation and the mechanical properties offibers, namely, the higher mechanical properties of PBIA fibers can be achieved by drawing.

Hydrogen bonding plays an important role in making polyamides engineering plastics. At the same time, to date, they have restricted the drawing processing in polyamides.[6] In addition to hydrogen bonding, crystallites also can limit further alignment of molecular chain.[6] In our research, we found that the by-product HCl, released during the polymerization process of PBIA fibers, can complex with PBIA fibers forming protonated PBIA fibers. The PBIA/HCl complex fibers are amorphous and the hydrogen bonding between C=N and NH of PABZ units also be broken. This knowledge opens up the possibility to deform the polymer and manipulate the molecular arrangements in the absence of crystallinity and hydrogen bonding. In this article, the diamine monomer 5-amino-2-(4-aminobenzene) benzimidazole was introduced into the main chain of PPTA and the PBIA was synthesized. The present study mainly focuses on the effect of PBIA–HCl complexation on fibers drawability. Due to the complexation of HCl with PBIA fibers which can break the hydrogen bonding between C=N and NH of PABZ units, and lead to an amorphous structure and a lower T_g, the two-step drawing–annealing processing technology is adopted to obtain higher mechanical properties. The results in this article may provide a novel access to solve the contradiction between high performance and good processability of PBIA fibers.

MATERIALS AND METHODS

Materials

Paraphthaloyl chloride (TPC), p-phenylenediamine (PDA), and LiCl were obtained from ChengDu Kelong Chemical Co., Ltd., and used as received. 5-Amino-2-(4-aminobenzene) benzimidazole (PABZ) was obtained from Changzhou Sunlight Medical Raw Material Co. Ltd., its chemical formula is shown in Figure 1. Dimethylacetamide (DMAC) was obtained from Shanghai Qunli Chemical Company and distilled over P_2O_5 under reduced pressure before use.

Synthesis of PBIA

A total of 350 g DMAC and 10.5 g dry LiCl were added into a 500 mL three-necked bottle and stirred. When LiCl was dissolved, 2.561 g (0.0237 mol) PDA and 5.313 g (0.0237 mol) PABZ were added and dissolved. After the mixture was cooled to 0–5°C in an ice bath in a nitrogen atmosphere, 9.629 g (0.0474 mol) TPC was added and rapidly stirred for 1 h. Further stirring was carried out at 30°C for 2 h and yellowish-brownorgano-soluble PBIA solution was obtained. Figure 2 shows the synthetic process and the chemical structure of the PBIA.

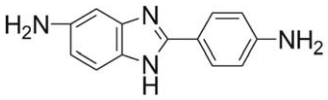

Figure 1. Molecular structural formula of PABZ.

Preparation of the PBIA Fibers

The resulting copolyamide solutions were filtered and degassed prior to use. Copolyamide fibers were eventually obtained by wet spinning and the detailed process was shown in our previous paper.[12] The coagulation bath was a mixture of water and DMAC. The obtained copolyamide fibers were washed in water at 80°C for 1 h in order to remove LiCl and residual solvents.

Hot Drawing

The hot-drawing experiments were carried out in a heated double-walled tube (length 1.5 m) at different temperatures in a nitrogen atmosphere. The same tension for all specimens can be controlled by the fiber winding machine. The hot drawing of PBIA/HCl complex fibers were carried out at 280°C, 300°C, 320°C, 340°C, and 360°C, respectively. After drawing, the specimens were all annealed by fixing the stretched fibers at 400°C.

Characterization

Thermogravimetric analysis (TGA) was performed under N_2 atmosphere at a heating rate of 10°C/min in the range of 50–800°C using the TA Instrument TGA-2950. The tensile mechanical properties of the fibers were measured using an Instron Model 5567 twin-column table-mounted testing system at ambient conditions with a gauge length of 215 mm and a displacement rate of 25 mm/min. Fourier transform infrared (FTIR) spectra of PBIA fibers were recorded on a Nicolet Magna 650 spectroscope in the range from 4000 to 400 cm^{-1}. Wide-angle X-ray diffraction (WAXD) analysis of copolyamide fibers was performed on a Philips X'Pert PRO MPD with 2θ ranging from 5° to 45°. The two-dimensional (2D) WAXD patterns were obtained using a Bruker D8 discovery X-ray diffractometer (40 kV, 40 mA). Small-angle X-ray scattering (SAXS) experiments were performed using a NanoSTAR-U (BRUKER AXS INC.) with Cu Kα radiation ($\lambda = 0.154$ nm). The generator was operated at 40 kV and 650 μA. Two-dimensional SAXS patterns were obtained using an HI-STAR detector. The sample-to-detector distances were $F = 1062$ mm. Thermal dynamic mechanical behavior of the prepared fiber was measured using a dynamic mechanical analysis (DMA) system of TA Q800

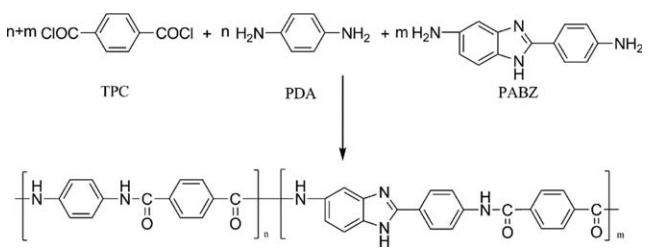

Figure 2. The synthetic process and the chemical structure of the copolyamide (m : n = 1 : 1)

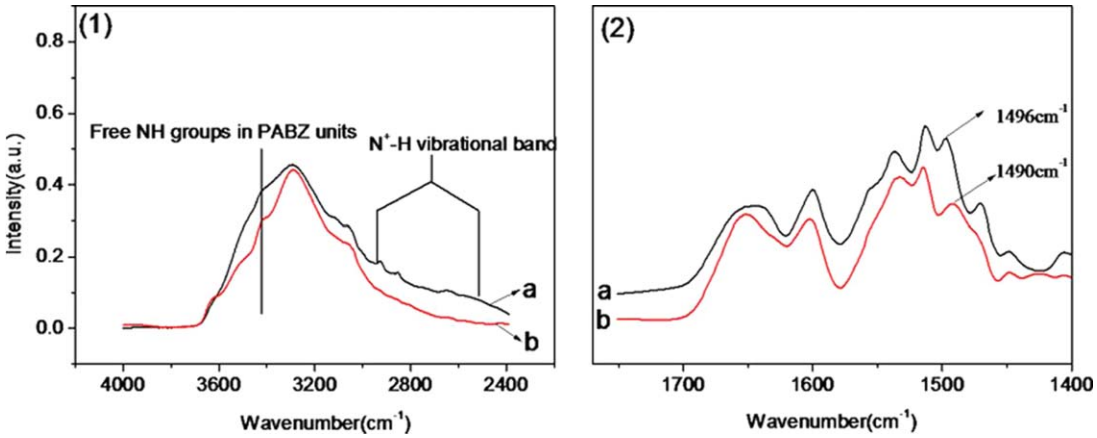

Figure 3. FTIR spectra of NH region (1); C=N region (2). The red line "a" represents the FTIR spectra of PBIA fibers, and black line "b" represents the FTIR spectra of PBIA/HCl complex fibers. [Color figure can be viewed in the online issue, which is available at wileyonlinelibrary.com.]

instrument under N_2 atmosphere at a heating rate of 10°C/min in the range of 30–340°C. The experimental sample was a single fiber and the load frequency was 1 Hz.

RESULTS AND DISCUSSION

Properties of As-Spun PBIA/HCl Complex and PBIA Fibers

As reported by Aharoni *et al.*,[13] the basic nitrogen sites of heterocycle such as benzimidazole act as strong proton acceptors with respect to HCl, thus forming protonic charge carriers. Due to the PABZ units contained in PBIA fibers, the PBIA fibers can also complex with HCl. In addition, from the FTIR spectra shown in Figure 3, bands can be seen at 3415 and 1490 cm^{-1}, which have been attributed to isolated, non-hydrogen bonded NH groups in PABZ units[14] and C=N stretching vibrations in PABZ units,[15,16] respectively. The ratio of I_{3415}/I_{3300} is used to characterize the change of non-hydrogen bonded NH group in benzimidazole units. Obviously, the ratio of I_{3415}/I_{3300} in PBIA/HCl complex fibers is significantly higher than that of PBIA fibers, which indicates that the non-hydrogen bonded NH groups in PBIA/HCl complex fibers are more than that of PBIA fibers. In addition, for PBIA/HCl complex fibers, C=N vibrational band of PABZ units shifts to higher frequency (blue shift from 1490 to 1496 cm^{-1}), due to the increment in bond order which is caused by the α-protonation effect in the simple heterocyclic species.[17] The very broad absorption band appearing around 2800 cm^{-1} can be attributed to Fermi resonance between the $\nu(N^+–H)$ mode and second harmonics of internal vibrations[14], which can also manifest that HCl complex with the C=N group of PABZ units. The schematic diagram is shown in Figure 4.

Song *et al.*[18] studied the relationship between glass transition temperature (T_g) and intermolecular interactions. Their results indicated that the values of T_g increased as a function of the content of hydrogen bonds interactions. The T_g is influenced by molecular chain rigidity, high intermolecular/intramolecular interactions, and chain packing density. Figure 5 shows the DMA curves (tan delta) of PBIA/HCl complex fibers and PBIA fibers. The temperature at the peak of the tan delta curve represents T_g of the macromolecular chains in amorphous domain, which are 254°C (PBIA/HCl complex fibers) and 276°C (PBIA fibers), respectively. For the PBIA/HCl complex fibers, complexed HCl may lead to the elimination of interchain hydrogen bonding, which provides a lower T_g. The lower T_g usually corresponds to the better processability.

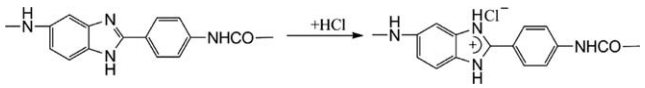

Figure 4. The schematic diagram of HCl complexing with PABZ units.

The Evolution of Structure and Performance for PBIA/HCl Complex Fibers During Hot Drawing Process at Different Temperature

The decomplexation of HCl can be achieved at high temperature and leads to the release of electron donor C=N in PABZ units, which may give rise to the change of hydrogen bonding, crystallinity, and T_g. So, the different content of HCl in PBIA/HCl complex fibers may lead to different drawability. The relation between remaining HCl content (the weight loss between 280°C and 360°C in TGA corresponds to the HCl content of PBIA/HCl complex fibers, which can be proved from the results in Figures S1 and S2 in the Supporting Information) in PBIA/

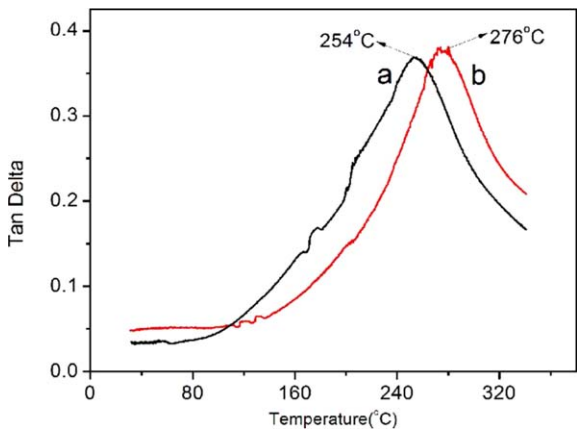

Figure 5. DMA curve of (a) PBIA/HCl complex fibers and (b) PBIA fibers. [Color figure can be viewed in the online issue, which is available at wileyonlinelibrary.com.]

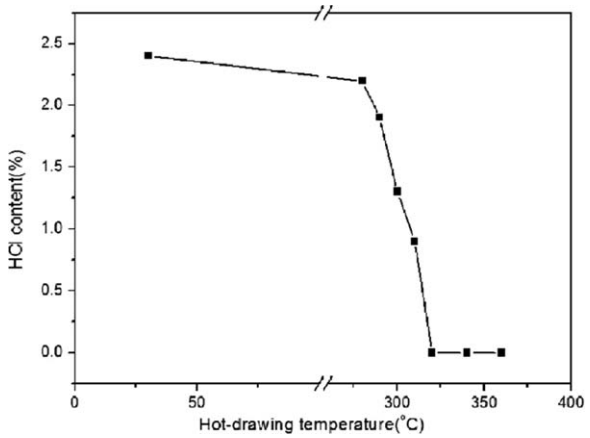

Figure 6. The residual HCl content of PBIA/HCl complex fibers drawn at different temperature.

HCl complex fibers and drawing temperature is shown in Figure 6. The remaining HCl content in PBIA/HCl complex fibers at room temperature is 2.4%. After drawn at 280°C, the remaining HCl content in PBIA/HCl complex fibers is 2.2%, which indicates that the complexation between PBIA fibers and HCl is stable, and will not be destroyed at this temperature. However, when the drawing temperature is above 280°C, the HCl content significantly decreases, and above 320°C there is no residual HCl in the fibers.

Hydrogen bonding plays an important role in making polyamides engineering plastics. At the same time, to date, they have restricted the drawing processing in polyamides. FTIR is an effective way to study hydrogen bonding interactions. FTIR spectra of PBIA/HCl complex fibers drawn at different temperature are shown in Figure 7. The NH stretching bands of amide and benzimidazole units are observed in the wavenumber interval from 3200 to 3500 cm^{-1}. The peak located between 1480 and 1490 cm^{-1} can be assigned to the stretching vibration of C=N in the benzimidazole ring.[15,16,19] The peak centered at 3415 cm^{-1} can be attributed to the stretching vibration of the

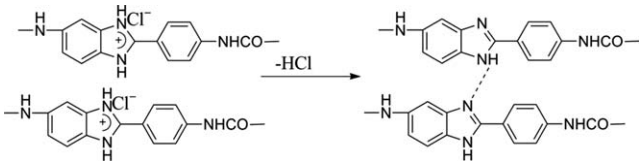

Figure 8. The proposed model for the formation of hydrogen bonding.

isolated, non-hydrogen bonded NH groups in benzimidazole units[14] and the peak centered approximately at 3300 cm^{-1} is related to the hydrogen bonded NH group.[14] In order to study the change of non-hydrogen bonded NH group in benzimidazole units during drawing process, the internal standard of hydrogen bonded NH stretching bands was introduced, and the ratio of I_{3415} to I_{3300} was used to characterize the change of non-hydrogen bonded NH group in the benzimidazole units. Obviously, the values of I_{3415}/I_{3300} significantly decrease when the drawing temperature is above 280°C, which indicates that the hydrogen bonding interactions become stronger. In addition, the C=N stretching band also obviously shifts to a lower wavenumber when the drawing temperature is above 280°C. As discussed above, when the drawing temperature is above 280°C, the HCl content significantly decreases. Therefore, combined with these results, it is reasonable to conclude that the decomplexation of HCl leads to the formation of hydrogen bonding between C=N and the NH groups at the site of benzimidazole rings, as schematically shown in Figure 8.

As the hot drawing of PBIA/HCl complex fibers was carried out at high temperature, thus it is necessary to study the stability of hydrogen bonding between C=N and the NH groups at high temperature. In situ FTIR studies of PBIA fibers (not complex with HCl) were carried out to evaluate the stability of hydrogen bonding at high temperature. The results are shown in Figure 9. It can be found that band position of $\nu_{(C=O)}$ stretching band shifts to higher wavenumbers with the increase of temperature, which indicates the hydrogen bonding interactions between C=O and NH become weakened. However, the peak position of ν(C=N) in benzimidazole stay unchanged, which indicates

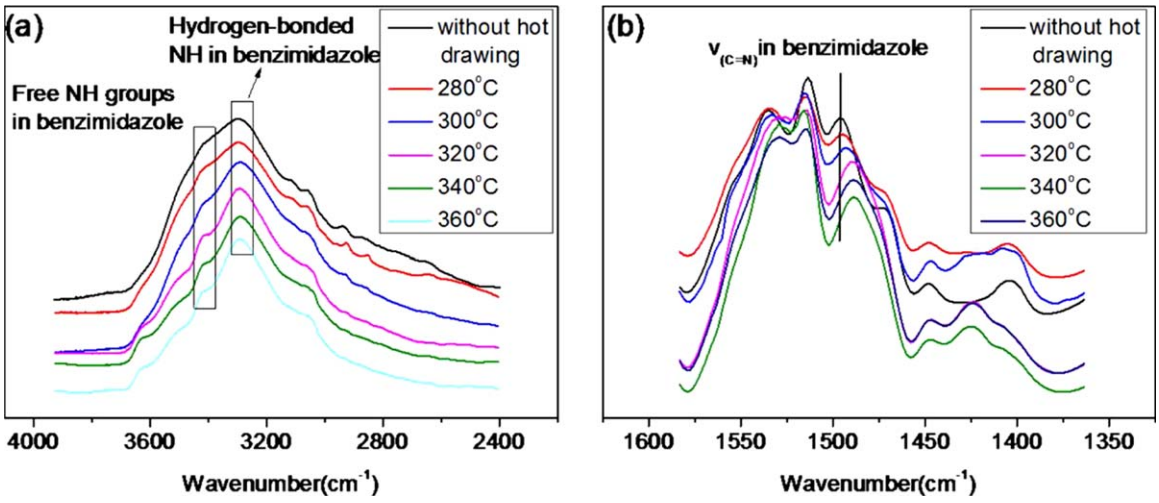

Figure 7. FTIR spectra of PBIA/HCl complex fibers after hot drawing at different temperature. The different colored lines indicate that PBIA fibers have been drawn at different temperature. [Color figure can be viewed in the online issue, which is available at wileyonlinelibrary.com.]

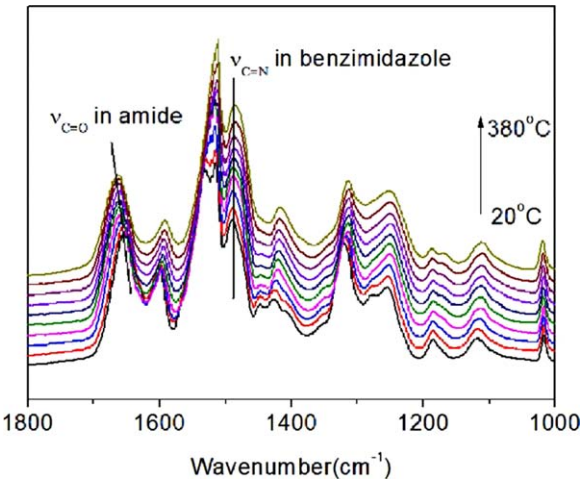

Figure 9. In situ FTIR spectra of PBIA fibers (not complex with HCl). [Color figure can be viewed in the online issue, which is available at wileyonlinelibrary.com.]

the hydrogen bonding between C=N and NH is stable in high temperature.

In addition, crystallites act like quasi-crosslinks during drawing, restricting the movement of molecular chain and limiting the control over polymer microstructure. The normalized WXRD patterns and curve-fitting deconvolution of the WAXD spectra in Figure 10 are presented to illustrate the evolution of the aggregation structure of PBIA/HCl complex fibers after drawing at different temperature. The as-spun fibers exhibit a broad peak at 20°–25°, representing an amorphous structure. For the fibers hot drawn at 280°C, one crystalline-like peak, which is expressed using a red line (peak a) in WAXD diffractograms, appears at 20.5°. At the hot drawing temperature above 280°C, another crystalline peak, which is expressed using a green line (peak b) in WAXD diffractograms, appears at about 23°. It is well known that the oriented PPTA fibers show two strong reflections at about 20° and 23° located on the equator, which correspond to the intermolecular hydrogen bonded sheets between the C=O and the N-H groups of the amide units and the $\pi-\pi$ stacking of benzene rings,[20,21] respectively. So it can be speculated that the PBIA fibers containing PPTA and PABZ units show similar crystal structure. In addition, a broad peak which is expressed using a blue line in WAXD diffractograms can be regarded as amorphous peaks. The crystallinity X_{cr} can be defined by the following equation:[22]

$$Xcr = \frac{\mathrm{Ac}}{\mathrm{Ac}+\mathrm{Aa}} \times 100\% \quad (1)$$

where Ac is crystallization peak area and Aa is the amorphous peak area. For PBIA/HCl complex fibers drawn at 280°C, the crystallinity is 8.4%. But for fibers drawn above 280°C, the crystallinity significantly increases a lot. The values of crystallinity for fibers hot drawing above 280°C are 30.5% (300°C), 40.3% (320°C), 41.3% (340°C), and 42.4% (360°C). It can be found that the crystallinity of PBIA fibers significantly increases during drawing between 280°C and 320°C (from 8.4% to 40.3%); however, when the drawing temperature is above 320°C, the crystallinity does not change much. The content of HCl sharply decreases from 2.2% to 0% during drawing at 280–320°C, during which a significant increase of crystallinity can also be observed, which indicates that the change of crystallinity may be related to HCl. In addition, the results obtained from Figures S4, S5, and S6 in Supporting Information show that when PBIA complexed with HCl, a significant change in structure can be found. Thus, we believe that the increase of crystallinity is related to the decomplexation of HCl, namely, HCl can suppress crystallization.

As discussed above, the decomplexation of HCl can be achieved above 280°C and the hydrogen bonding and crystallinity also significantly improved. The hydrogen bonding and

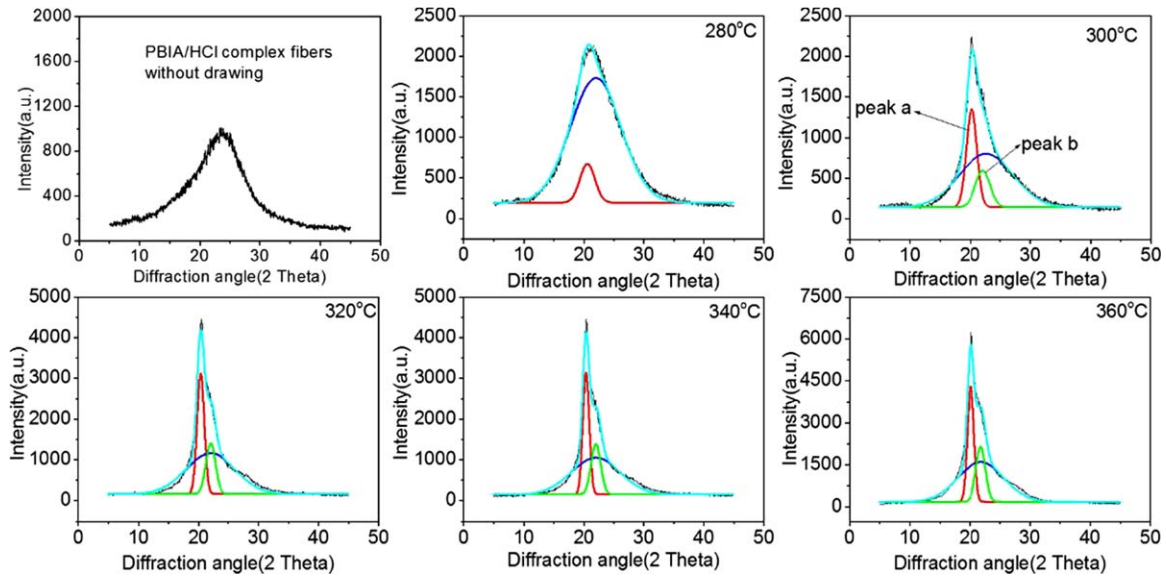

Figure 10. WAXD spectra and corresponding curve-fitting deconvolution of PBIA/HCl complex fibers through drawn at different temperature. [Color figure can be viewed in the online issue, which is available at wileyonlinelibrary.com.]

Table I. The Mechanical Properties of Different Processed Fibers

Sample	Tensile strength (cN/dtex)	Initial modulus (cN/dtex)	Elongation to break (%)
Two-step drawn-annealed PBIA/HCl complex fibers			
$280_{(2.2\%\ HCl)}-400$	29.1 (±0.65)[a]	760 (±6.56)[a]	3.87 (±0.09)[a]
$300_{(1.3\%\ HCl)}-400$	27.3 (±0.72)[a]	737 (±6.84)[a]	4.09 (±0.08)[a]
$320_{(0\%\ HCl)}-400$	25.2 (±0.71)[a]	716 (±5.12)[a]	4.18 (±0.10)[a]
$340_{(0\%\ HCl)}-400$	24.6 (±0.62)[a]	700 (±4.15)[a]	4.21 (±0.07)[a]
$360_{(0\%\ HCl)}-400$	24.1 (±0.32)[a]	695 (±3.31)[a]	4.17 (±0.05)[a]
One-step processed PBIA/HCl complex fibers			
400-Drawing	24.2 (±0.48)[a]	708 (±3.16)[a]	4.15 (±0.06)[a]
400-Annealing	25.3 (±0.58)[a]	704 (±6.13)[a]	4.26 (±0.05)[a]
Two-step drawn-annealed PBIA fibers(not complex with HCl)[b]			
280-400	22.4 (±0.31)[a]	672 (±1.58)[a]	4.38 (±0.03)[a]

[a] Standard deviation and 5 data points were collected for per sample.
[b] Removing the HCl from PBIA solution at a low temperature can be achieved by adding $LiCO_3$.

crystallization would limit the movement of molecular chain and lead to the improvement of T_g, which is not conducive to the drawing of fibers. In addition, the HCl can act as a kind of plasticizer, and the release of HCl can also lead to the decrease of processability for PBIA fibers. Therefore, 280°C is the best drawing temperature, and drawing temperature above 280°C may not be good for the orientation of molecular chain along the drawing direction.

Properties of Different Processed PBIA Fibers

The mechanical properties of different processed fibers are shown in Table I. First, for the two-step drawn-annealed PBIA/HCl complex fibers, both tensile strength and initial modulus decreased monotonously with an increase in the drawing temperature. The HCl content in PBIA/HCl fibers decrease with increasing in drawing temperature, and the removal of HCl leads to the reform of hydrogen bonding and crystallization, which may causing the deterioration of drawability; therefore the decrease of tensile strength may be due to the formation of hydrogen bonding and crystallization during the decomplexation of HCl, and the fibers which are drawn at 280°C and subsequently annealed at 400°C possess a highest tensile strength of 29.1 cN/dtex and a modulus of 745 cN/dtex. However, the traditional one-step drawn PBIA/HCl complex fibers at 400°C only have tensile strength at break 24.2 cN/dtex, which is lower than that of annealed fibers, and the decrease of tensile strength may be because of the reason that when the drawing temperature is at 400°C, the hydrogen bonding and crystallization caused by the decomplexation of HCl limit the mobility of molecular chain and may lead to the break of some fibrils. In addition, if we first removed the HCl in PBIA solution, the PBIA fibers (not complex with HCl) can be obtained. However, the tensile

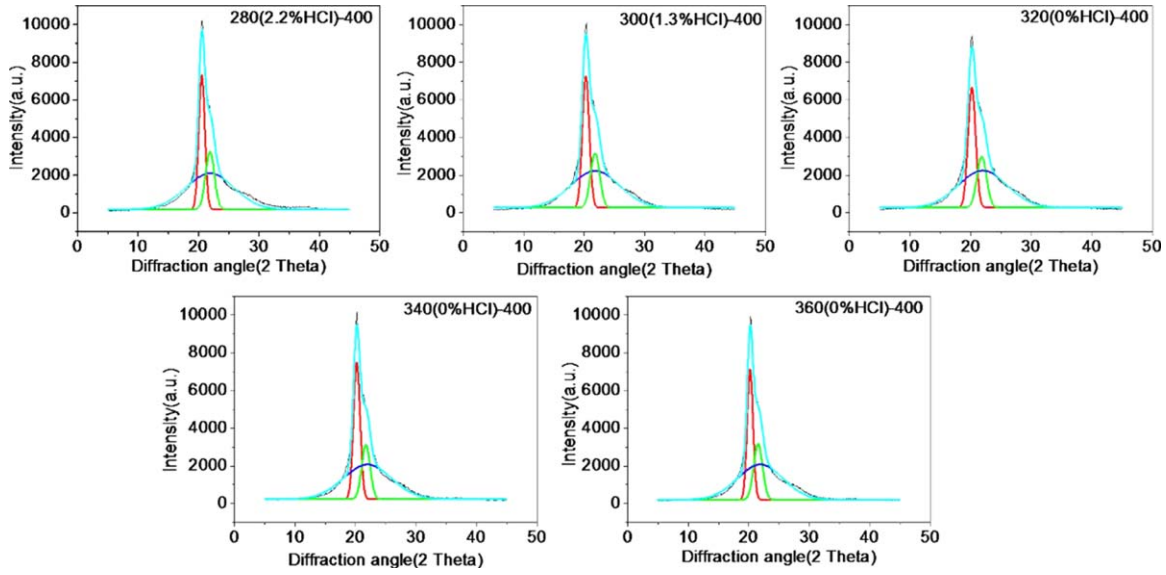

Figure 11. WAXD curves of the two-step drawn-annealed PBIA/HCl complex fibers. [Color figure can be viewed in the online issue, which is available at wileyonlinelibrary.com.]

Table II. The Lateral Size of L_a and L_b

Sample	σ_a	σ_b	L_a(nm)	L_b(nm)
$280_{(2.2\%\ HCl)}-400$	0.0206	0.0150	6.84	9.40
$300_{(1.3\%\ HCl)}-400$	0.0234	0.0161	6.37	8.94
$320_{(0\%\ HCl)}-400$	0.0218	0.0154	6.45	9.23
$340_{(0\%\ HCl)}-400$	0.0228	0.0150	6.35	9.41
$360_{(0\%\ HCl)}-400$	0.0209	0.0152	6.73	9.30

strength of two-step drawn-annealed PBIA fibers is 22.4 cN/dtex, which is far lower than that of the two-step drawn-annealed PBIA/HCl complex fibers.

As we know, the mechanical properties of fibers depend mainly on the crystallinity and orientation. The aggregation structure of two-step drawn-annealed PBIA/HCl complex fibers was measured by WAXD. As shown in Figure 11, the WAXD curves of the drawn-annealed fibers can be fitted into two crystallization peak and an amorphous peak (the curve-fitting deconvolution method is the same as that of Figure 10), and the crystallinity X_{cr} can be calculated by eq. (1). As a result, the crystallinity is almost the same for the drawn-annealed fibers, and the values of crystallinity of $280_{(2.2\%\ HCl)}-400$, $300_{(1.3\%\ HCl)}-400$, $320_{(0\%\ HCl)}-400$, $340_{(0\%\ HCl)}-400$, and $360_{(0\%\ HCl)}-400$ are 43.4%, 43.8%, 43.5%, 44.1%, and 43.9%, respectively.

In addition, in order to deeply analyze and discuss the crystallite size of PBIA fibers, the lateral size of the ordered structures corresponding to the two peaks is evaluated by Scherrer's equation[23], as given below:

$$L = \frac{K\lambda}{\sigma\cos\theta}$$

where L is the correlation length of the ordered structure, $\lambda$is the X-ray wavelength, σ is the half-width at half-maximum in radians for the diffraction peak, and K is the constant around 0.9. Table II shows the domain size of L_a (ordered structures corresponding to peak a in red line can be regarded as intermolecular hydrogen bonding sheets between the C=O and the N-H groups of the amide units) and L_b (ordered structures corresponding to peak b in green line cause by $\pi-\pi$ stacking of benzene rings). It can be found that L_a and L_b change only a little with the change of drawing temperature. In addition, according to the above result that the crystallinity is almost the same for the different drawn-annealed fibers, thus, it is reasonable to conclude that the different mechanical properties of two-step drawn-annealed PBIA/HCl complex fibers are not caused by crystallinity and correlation length of the ordered structure.

Generally, the mechanical properties of fibers are strongly influenced by orientation. Drawing is an effective method to enhance the orientation degree of fibers. Orientation degree can be obtained by 2D WAXD. The 2D WAXD diffraction patterns which exhibit strong equatorial reflections indicating good packing along the fiber axis and high molecular orientation are shown in

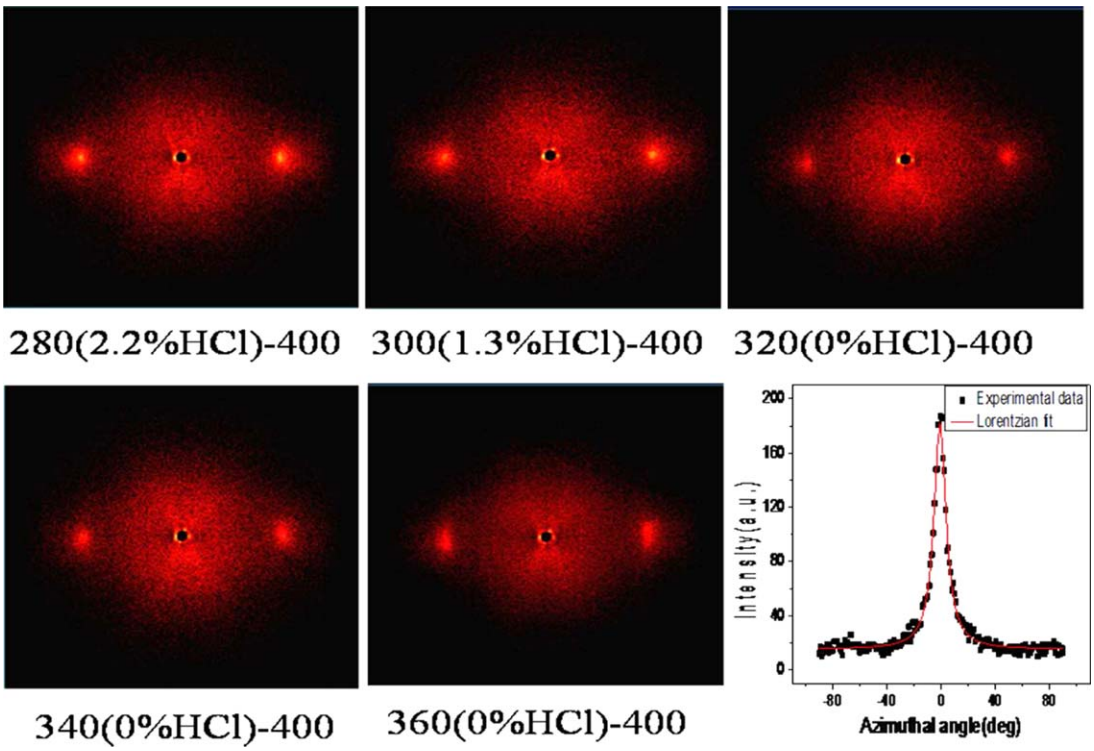

Figure 12. The 2D WAXD diffraction patterns of PBIA/HCl complex fibers drawn at different temperature and subsequently annealed at 400°C, and a representative azimuthal intensity $I(\phi)$ profile of the reflection and its Lorentzian fit overlaid with the azimuthal intensity data (lower right). [Color figure can be viewed in the online issue, which is available at wileyonlinelibrary.com.]

Table III. Results of Various Parameters and Orientation Factor f_2

Sample	$\int_0^{\frac{\pi}{2}} I(\phi)\cos^2\phi\sin\phi d\phi$	$\int_0^{\frac{\pi}{2}} I(\phi)\sin\phi d\phi$	$\overline{\cos^2\phi}$	f_2
$280_{(2.2\%\ HCl)}-400$	9.82	10.35	0.94	0.92
$300_{(1.3\%\ HCl)}-400$	10.90	11.64	0.93	0.90
$320_{(0\%\ HCl)}-400$	5.07	5.47	0.92	0.89
$340_{(0\%\ HCl)}-400$	10.89	11.91	0.91	0.87
$360_{(0\%\ HCl)}-400$	12.57	13.86	0.90	0.86

Figure 12. For the fibers, the degree of orientation, expressed as $\overline{\cos^2\phi}$, can be calculated using the following equation:[11]

$$\overline{\cos^2\phi}=\frac{\int_0^{\pi/2} I(\phi)\cos^2\phi\sin\phi d\phi}{\int_0^{\pi/2} I(\phi)\sin\phi d\phi} \quad (2)$$

where ϕ is the azimuthal angle and $I(\phi)$ is the scattering intensity for the angle ϕ. Frequently, the parameter f_2, the so-called Herman's orientation function, is used to describe the degree of orientation:

$$f_2=\frac{3\overline{\cos^2\phi}-1}{2} \quad (3)$$

A representative azimuthal intensity profile of the reflections is shown on the lower right of Figure 12. The variation of various parameters and orientation factor f_2 with the change of drawing temperature (namely, different HCl content in fibers) in PBIA/HCl complex fibers is illustrated in Table III. The degree of orientation is found to decrease with increasing drawing temperature. The fibers which are drawn at 280°C and subsequently annealed at 400°C have the highest value of orientation degree, which indicates that drawing below decomplexation temperature of HCl is helpful for the orientation of molecular chain along the fiber axis. Above 280°C, the decomplexation of HCl leads to the formation of hydrogen bonds, crystallization, and improve the T_g, which hinders the mobility of molecular chain during drawing process. As discussed above, the crystallinity is almost the same for the drawn-annealed PBIA/HCl complex fibers. So, the different mechanical properties of drawn-annealed PBIA/HCl complex fibers should be caused by the different orientation.

In the following section, we intend to illustrate the corresponding morphological changes extracted by the SAXS. Figure 13

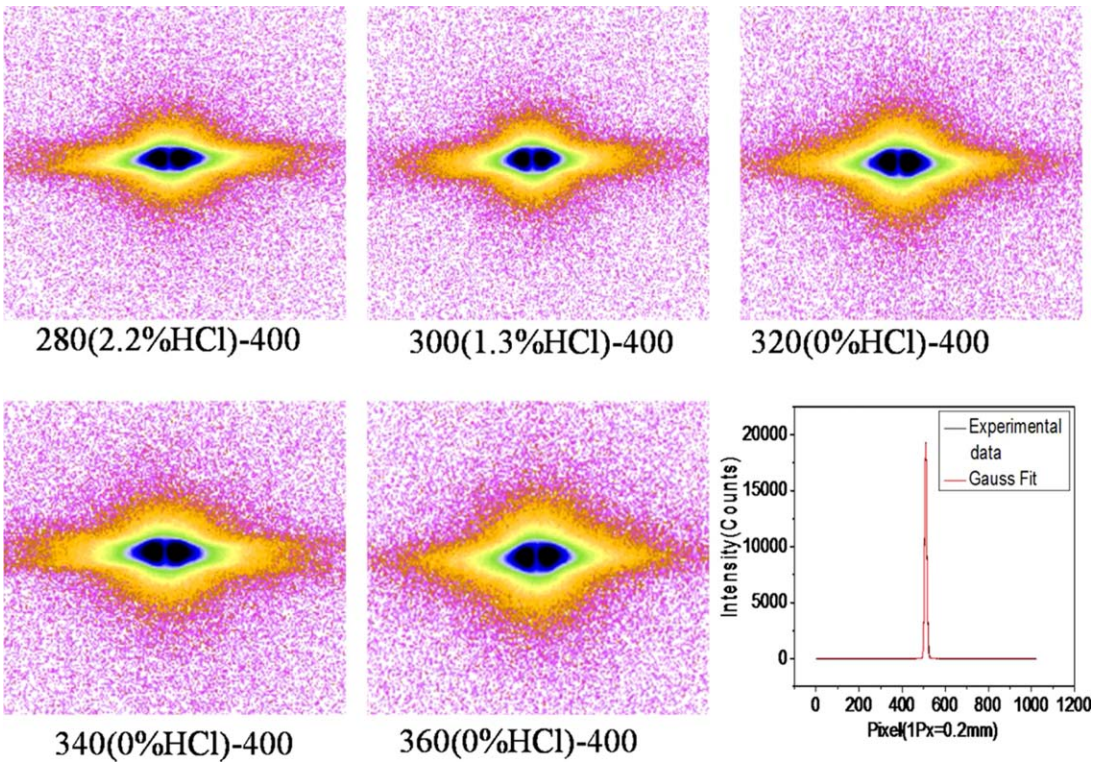

Figure 13. The 2D SAXS patterns of two-step drawn-annealed PBIA/HCl complex fibers and a representative equatorial scan. [Color figure can be viewed in the online issue, which is available at wileyonlinelibrary.com.]

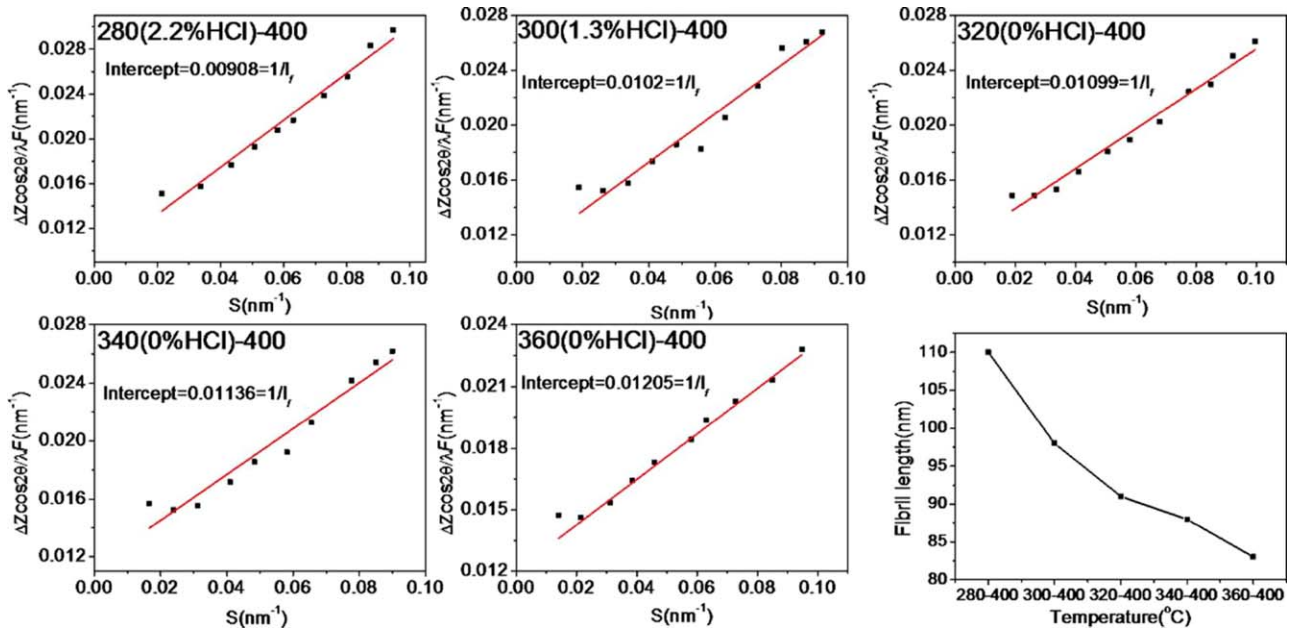

Figure 14. The axial integral breadths of equatorial reflections plotted as a function of the scattering vector s and the fibril length of the two-step drawn-annealed PBIA/HCl complex fibers at different drawing temperature. [Color figure can be viewed in the online issue, which is available at wileyonlinelibrary.com.]

shows the 2D SAXS patterns of the two-step drawn-annealed PBIA/HCl complex fibers and a representative equatorial scan. The common feature seen in these patterns is that the SAXS intensity has a shape of a streak along the equator and there is no detectable scattering along the meridional direction. The streak pattern indicates that the superstructure of the PBIA fibers is mainly a fibrillar structure, with no trace of lamellar morphology. The streak on the equator is produced by scattering objects extended along the fibers direction. We have used the following method proposed by David[24] to analyze the intensity distribution in order to obtain the information of the average fibril length. The fibril length (l_f) can be obtained using the following equation:[24,25]

$$\frac{\Delta Z\cos 2\theta}{\lambda F} = \frac{1}{2l_f} + \left[\frac{1}{4l_f^2} + s^2\sin^2\beta_f\right]^{1/2} \quad (4)$$

where ΔZ is the integral width which can be obtained from equatorial scan, $s = (2\sin\theta)/\lambda$, 2θ is the scattering angle, λ is the X-ray wavelength, F is the detector to fiber distance, l_f is the length of the fibrils, and β_f is the misorientation of the normals to the Bragg planes from the equator. The fibril length (l_f) thus could be obtained from the intercept of the $\Delta Z\cos 2\theta/\lambda F$ vs. s.

Figure 14 show the axial integral breadths of equatorial reflections plotted as a function of the scattering vector s and the fibril length of the two-step processed PBIA fibers. It is seen that the fibril length decreased with decreasing in HCl content (increasing the drawn temperature). During the drawing process of fibers, some amorphous phase can be straightened out, which leads to the increase of fibril length[11,26]. So, the gradually reduced fibril length can indicate that the drawing above the decomplexation temperature of HCl is not conducive to obtain the high orientation and mechanical properties of fibers and the decomplexation of HCl may leads to the decrease of drawability.

CONCLUSIONS

Due to the PABZ units contained in PBIA fibers, the PBIA fibers can complex with HCl. The PBIA/HCl complex fibers are amorphous, and the hydrogen bonding between C=N and NH of PABZ units also be broken in PBIA/HCl complex fibers. The PBIA/HCl complex fibers provide a way to temporarily suppress the effects of hydrogen bonds and crystallinity, which allow a potential increase in orientation during drawing process, and then, upon decomplexation/regeneration, to restore hydrogen bonding and crystallization, resulting in higher mechanical properties. Therefore, the as-spun fibers were drawn first at 280°C higher than Tg of the PBIA/HCl complex fibers and lower than decomplexed temperature of HCl, which temporarily suppresses the formation of hydrogen bonding and crystallization. Subsequently, the fibers were annealed at 400°C to regenerate hydrogen bonding between PABZ units and crystallization. However, when the drawing was carried out above the decomplexation temperature of HCl, the mechanical properties of the drawn-annealed PBIA/HCl complex fibers decreased with a decrease in the HCl content of fibers. The crystallinity for these fibers is almost the same. The different mechanical properties of the drawn-annealed PBIA/HCl complex fibers at different drawing temperature are mainly due to the different orientation. The result of SAXS also can indicate that the decomplexation of HCl may lead to the decrease of drawability.

ACKNOWLEDGMENTS

This work was financially supported by the National Natural Science Foundation of China (Grant No.50973073) and State Key

Laboratory of Polymer Materials Engineering (Grant No. sklpme 2014-2-04). The authors acknowledge Analytical & Testing Centre of Sichuan University, People's Republic of China for characterization.

REFERENCES

1. Kotek, R.; Jung, D.; Tonelli, A.; Vasanthan, N. *J. Macromol. Sci. C* **2005**, *45*, 201.
2. Yang, Z.; Yin, H.; Li, X.; Liu, Z.; Jia, Q. *J. Appl. Polym. Sci.* **2010**, *118*, 1996.
3. Li, B.; Pang, Y.; Fan, C.; Gao, J.; Wang, X.; Zhang, C.; Liu, X. *J. Appl. Polym. Sci.* **2014**, 131.
4. Yao, J.; Luo, L.; Wang, X.; Li, K.; Huang, J.; Gao, J.; Li, B.; Wang, H.; Zhang, C.; Liu, X. *J. Polym. Res.* **2014**, *21*, 1.
5. Nishimura, H.; Donkai, N.; Miyamoto, T. *J. Polym. Sci. Part A: Polym. Chem.* **1998**, *36*, 3045.
6. Afshari, M.; Gupta, A.; Jung, D.; Kotek, R.; Tonelli, A.; Vasanthan, N. *Polymer* **2008**, *49*, 1297.
7. Vasanthan, N.; Kotek, R.; Jung, D.-W.; Shin, D.; Tonelli, A. E.; Salem, D. R. *Polymer* **2004**, *45*, 4077.
8. Downing, J. W.; Newell, J. A. *J. Appl. Polym. Sci.* **2004**, *91*, 417.
9. Zhang, S.-h.; He, G.-q.; Liang, G.-z.; Cui, H.; Zhang, W.; Wang, B. *Appl. Surf. Sci.* **2010**, *256*, 2104.
10. Berrada, M.; Carriere, F.; Abboud, Y.; Abourriche, A.; Benamara, A.; Lajrhed, N.; Kabbaj, M. *J. Mater. Chem.* **2002**, *12*, 3551.
11. Ran, S.; Fang, D.; Zong, X.; Hsiao, B.; Chu, B.; Cunniff, P. *Polymer* **2001**, *42*, 1601.
12. Luo, L.; Yao, J.; Wang, X.; Li, K.; Huang, J.; Li, B.; Wang, H.; Liu, X. *Polymer* **2014**, *55*, 4258.
13. Aharoni, S. M.; Signorelli, A. J. *J. Appl. Polym. Sci.* **1979**, *23*, 2653.
14. Bouchet, R.; Siebert, E. *Solid State Ionics* **1999**, *118*, 287.
15. Xia, A.; Lü, G.; Qiu, X.; Guo, H.; Zhao, J.; Ding, M.; Gao, L. *J. Appl. Polym. Sci.* **2006**, *102*, 5871.
16. Xia, A.; Guo, H.; Qiu, X.; Ding, M.; Gao, L. *J. Appl. Polym. Sci.* **2006**, *102*, 1844.
17. Casabianca, L. B.; de Dios, A. C. *J. Phys. Chem. A* **2006**, *110*, 7787.
18. Song, G.; Zhang, Y.; Wang, D.; Chen, C.; Zhou, H.; Zhao, X.; Dang, G. *Polymer* **2013**, *54*, 2335.
19. Sun, N.; Liang, Y.; Xu, Z.; Li, H.; Shaohua, J.; Yibiao, L. *J. Polym. Eng.* **2013**, *33*, 337.
20. Mooney, D.; MacElroy, J. *J. Chem. Phys.* **1999**, *110*, 11087.
21. Haraguchi, K.; Kajiyama, T.; Takayanagi, M. *J. Appl. Polym. Sci.* **1979**, *23*, 915.
22. Sengupta, R.; Tikku, V.; Somani, A. K.; Chaki, T. K.; Bhowmick, A. K. *Radiat. Phys. Chem.* **2005**, *72*, 625.
23. Fukuda, M.; Kawai, H. *J. Polym. Sci. Part B: Polym. Phys.* **1997**, *35*, 1423.
24. Grubb, D. T.; Prasad, K. *Macromolecules* **1992**, *25*, 4575.
25. Wu, J.; Schultz, J. M.; Samon, J. M.; Pangelinan, A. B.; Chuah, H. H. *Polymer* **2001**, *42*, 7161.
26. Murthy, N.; Bednarczyk, C.; Moore, R.; Grubb, D. *J. Polym. Sci. Part B: Polym. Phys.* **1996**, *34*, 821.